Vol 18 No 3, March 2009
1674-1056/2009/18(03)/1116-07
Chinese Physics B
© 2009 Chin. Phys. Soc.
and IOP Publishing Ltd

Zero dispersion wavelength and dispersion slope control of hollow-core photonic bandgap fibres*

Zhang Hu(张 虎)†, Yang Bo-Jun(杨伯君), Liu Yu-Min(刘玉敏),
Wang Qiu-Guo(王秋国), Yu Li(于 丽), and Zhang Xiao-Guang(张晓光)

School of Science, Key Laboratory of Communication and Lightwave Technologies Ministry of Education, Beijing University of Posts and Telecommunications, Beijing 100876, *China*

(Received 20 June 2008; revised manuscript received 1 September 2008)

This paper investigates the zero dispersion wavelength and dispersion slope control of hollow-core photonic bandgap fibres (PBGFs) by using a full-vector finite element method. By simulation we found that theoretically the zero dispersion wavelength can be tailored by respectively changing the rounded diameter of air holes, pitch, refractive index, normalized thickness of core rings, and hole diameter to pitch ratio. At the same time the tailoring of dispersion slope can also be realized by changing the rounded diameter of air holes or pitch or normalized thickness of core rings. To illustrate the reasonability of fibre designs, this paper also gives the variance of normalized interface field intensity which measures the scattering loss relatively versus wavelength for different designs. From the viewpoint of loss, varying the rounded diameter and the thickness of core ring could shift zero wavelength but it is difficult to get the required parameters within so tiny range in practical drawing of PBGFs, on the other hand, it is possible in practice to respectively alter the pitch and refractive index to shift zero wavelength. But varying hole diameter to pitch ratio is not worthwhile because they each induce large increase of loss and narrowness of transmission bandwidth. The zero dispersion wavelength can be engineered by respectively varying the rounded diameter of air holes, pitch, refractive index, and normalized thickness of core rings without incurring large loss penalties.

Keywords: hollow-core photonic bandgap fibre, dispersion, full-vector finite element method, photonic crystal fibre

PACC: 4281, 4281D, 4230Q, 7820P

1. Introduction

Unlike the conventional fibres and index guiding photonic crystal fibres, the hollow-core photonic bandgap fibres(HC-PBGFs) guide light not via total internal reflection but through the trapping of light in an air core defect by an out-of plane photonic band gap (PBG),[1−4] so this kind of fibres exhibit a host of novel and unusual transmission properties, for example, lower Rayleigh scattering, lower nonlinearity, potentially lower transmission loss, higher optical damage thresholds, and longer interaction lengths with gas or liquid, and they can be used to study gas-based nonlinear optics,[5] high power delivery, soliton transmission,[6] pulse compression,[7] particle guidance[8] etc. As is widely known, the dispersion characteristics is a key factor for the application of fibres , and especially for the microstructured optical fibres, the control of dispersion plays an important role in the practical applications such as optical communication systems, dispersion compensation and nonlinear optics. The control of dispersion for photonic crystal fibres (PCFs) have been realized,[9,10] but for the HC-PBGFs, it does not come true yet, and further study is still needed to obtain the knowledge of the dispersion characteristics of HC-PBGFs.

This paper studied the waveguide group velocity dispersion dependence on the geometric parameters, such as rounded diameter of air holes, pitch, normalized thickness of core rings, the refractive index, and the hole diameter to pitch ratio. Because material dispersion contributes less to the total dispersion in HC-PBGFs with higher air-filling fraction,[10,11] the dispersion in HC-PBGFs could be controlled by properly changing the above mentioned parameters. Simulation shows that the zero dispersion wavelength and the dispersion slope can be engineered in such fibres.

*Project supported by the National Natural Science Foundation of China (Grant No 60578043) and the Beijing Education Committee Common Build Foundation (Grant No XK100130637).
†Corresponding author. E-mail: zhh309@sina.com

2. Fibre structure and modelling method

2.1. Fibre structure

Figure 1 shows the simulated cross sections of a 7 cells core HC-PBGF. The structure is an ideal representation of HC-PBGFs can be manufactured by the stack-and-draw method. The schematic simulated structure of the HC-PBGF is shown in Fig.1(a). The periodic hexagonal holes with rounded corners are arranged on a triangular cladding to form the photonic crystal. In Fig.1(a), d is the hole diameter, Λ is the hole pitch (centre-to-centre distance between the holes), d_c is the rounded diameter of a hexagon, d_p and d_q are the rounded diameter of a pentagon and the rounded diameter of a dodecagon silica ring surrounding the air core respectively, t_r is the thickness of the silica ring, the normalized thickness is considered as $T = t_r/(\Lambda - d)$, in order to exhibit a legible core ring, $T = 1$ is set in Fig.1. The background material is silica with index of 1.45. The cladding has 7 rings, and the core region is formed by the removal of 7 central holes in order to create the mode-guiding defect as illustrated in Fig.1(b). Figure 1(b) shows the simulated HC-PBGF with parameters of $d/\Lambda = 0.98$, $d_c/d = 0.45$, $d_p/\Lambda = 0.2$, $d_q/\Lambda = 1.1$, $t_r/(\Lambda - d) = 0.5$, and $\Lambda = 4.7\,\mu$m, air-filling fraction is 94.23%.

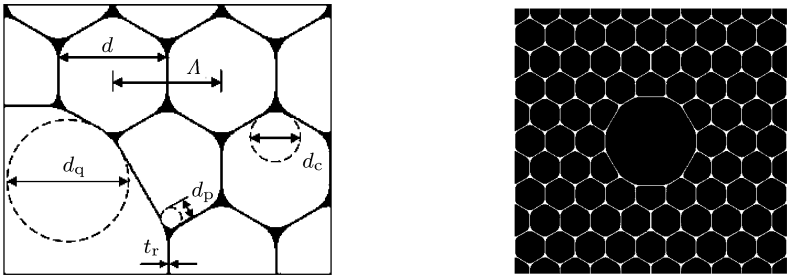


Fig.1. (a) Main parameters for the definition of the simulated structure: $d/\Lambda = 0.98$, $d_c/d = 0.45$, $d_p/\Lambda = 0.2$, $d_q/\Lambda = 1.1$, $t_r/(\Lambda - d) = 1$, and $\Lambda = 4.7\mu$m, air-filling fraction is 94.23%. (b) Cross section of the simulated HC-PBGF.

Figure 2 shows the modal dispersion curve for hole diameter to pitch ratio $d/\Lambda = 0.98$ as a function of normalized wavelength λ/Λ for HC-PBGF shown in Fig.1. The fundamental mode exists inside the PBG region and the lower and higher cutoff wavelengths are $\lambda/\Lambda \cong 0.2907$ and $\lambda/\Lambda \cong 0.3609$ respectively. The fibre operates in 1.50 μm wavelength range.

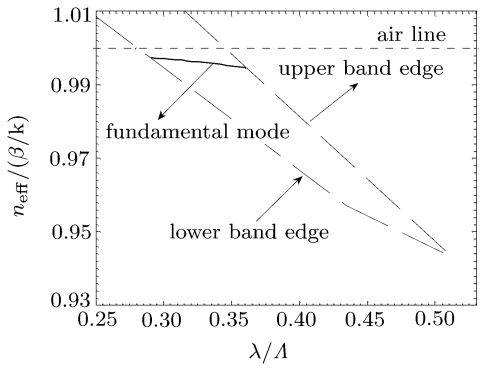


Fig.2. Modal dispersion curve of the fundamental mode as a function of normalized wavelength for HC-PBGF in Fig.1.

2.2. Modelling method

Because PCFs have a higher refractive index difference and do not satisfy the condition of weak-guide approximation, a vector method should be applied to obtain more accurate solution. A full-vector finite element method (FEM)[12,13] is one of such methods to effectively solve the problem of the waveguide, and it has already proven to be a fast and accurate tool for simulating micro-structured fibres. From the Maxwell's equations, the vector wave equation of the magnetic field vector $\boldsymbol{H}$ can be written as

$$\nabla \times (n^{-2}\nabla \times \boldsymbol{H}) - k_0^2 = 0, \tag{1}$$

where n and k_0 are the refractive index and the free space wave number, respectively. Assuming that the magnetic field can be decomposed into a slowly z-varying vector envelope $\boldsymbol{h}_t$ and a fast oscillating phase term $\exp(-\mathrm{j}\beta z)$, where β is the propagation constant. Substituting the two decompositions into Eq.(1) and using the zero divergence condition of the magnetic field $\nabla \cdot \boldsymbol{H} = 0$, we obtain the varying transverse mag-

netic field envelope equation

$$\frac{1}{n^2}\frac{\partial^2 \boldsymbol{h}_t}{\partial z^2} - 2\mathrm{j}\beta\frac{1}{n^2}\frac{\partial \boldsymbol{h}_t}{\partial z} + \frac{1}{n^2}\nabla_t(\nabla_t \cdot \boldsymbol{h}_t) - \nabla_t\left[\frac{1}{n^2}(\nabla_t \times \boldsymbol{h}_t)\cdot \hat{e}_z\right] \times \hat{e}_z + \left(k_0^2 - \frac{\beta^2}{n^2}\right)\boldsymbol{h}_t = 0, \quad (2)$$

where $\hat{e}_z$ is the unit vector in z direction. Using the Galerkin method, we can derive the following non-paraxial vector wave equation

$$[\boldsymbol{M}]\frac{\mathrm{d}^2\{\boldsymbol{h}_t\}}{\mathrm{d}z^2} - 2\mathrm{j}\beta[\boldsymbol{M}]\frac{\mathrm{d}\{\boldsymbol{h}_t\}}{\mathrm{d}z} + ([\boldsymbol{K}] - \beta^2[\boldsymbol{M}])\{\boldsymbol{h}_t\} = \{0\}, \quad (3)$$

where $\{\boldsymbol{h}_t\}$ is a column vector containing all the nodal values of the slowly varying transverse magnetic field components, $\{0\}$ is a null column vector, and $[\boldsymbol{M}]$ and $[\boldsymbol{K}]$ are the global element matrices including the contributions from all elements as shown in Ref.[12]. Considering the loss of optical fibre, we obtain the eigenvalue equation

$$[\boldsymbol{K}]\{\boldsymbol{h}_t\} = \beta^2[\boldsymbol{M}]\{\boldsymbol{h}_t\}. \quad (4)$$

Perfect matched layers are used as boundary condition. Mode distribution and modal propagation constant β can be obtained by solving the above equation. Accordingly, modal effective refractive index n_{eff} can be given as

$$n_{\mathrm{eff}} = \frac{\mathrm{Re}(\beta)}{k_0}, \quad (5)$$

where $\mathrm{Re}(\beta)$ means the real part of β. So the waveguide group velocity dispersion (GVD) D_{g} could be obtained by the following equation:

$$D_{\mathrm{g}} = -\frac{\lambda}{c}\frac{\mathrm{d}^2 n_{\mathrm{eff}}}{\mathrm{d}\lambda^2}, \quad (6)$$

where c is the velocity of light in a vacuum.

The loss is an important parameter to design a HC-PBGF. Away from anticrossing wavelengths, the domain factor of loss in PBGFs is the scattering loss due to roughness at the glass/air interface.[14−16] This loss is proportional to an overlap integral of the fundamental mode with the silica surfaces

$$F = \left(\frac{\varepsilon_0}{\mu_0}\right)^{\frac{1}{2}} \frac{\oint_{\text{hole perimeters}} |\boldsymbol{E}|^2 \,\mathrm{d}l}{\int_{\text{cross section}} |\boldsymbol{E}\times\boldsymbol{H}^*|\cdot\hat{e}_z \mathrm{d}S}, \quad (7)$$

where $\boldsymbol{E}$ and $\boldsymbol{H}$ are the electric and magnetic field of the fundamental mode and $\hat{e}_z$ is the unit vector along the fibre. In the following sections we assess the quality of designs of different fibres by using the factor F of the fundamental mode.

3. Zero dispersion wavelength and dispersion slope control

The dispersion properties of different designs of HC-PBGFs have been studied extensively in the following. We expect to tailor the chromatic dispersion of such fibres by manipulating the geometry of the core ring and the cladding. The dispersion D_{c} can be given as an approximate expression $D_{\mathrm{c}} \approx D_{\mathrm{m}} + D_{\mathrm{g}}$, where D_{m} is the material dispersion. For HC-PBGFs with higher air-filling fraction, D_{m} was calculated by using the method in Ref.[11] to find that it was much smaller than D_{g}, it was not considered in our calculation. By changing one of geometric parameters, such as d_{c}, Λ, n, T and d/Λ, while keeping others the same, the dependence of D_g on the above geometric parameters was studied, and the dispersion properties of fundamental modes were presented. To reduce the amount of surface modes as far as possible and be free from anticrossings between fundamental modes and surface modes, thin silica core rings[17,18] were adopted in our calculation. It was found that zero dispersion wavelength λ_0 could be controlled by varying one of the above parameters of HC-PBGFs.

Figures 3(a) and 3(b) show the dispersion variance as a function of wavelength, the normalized rounded diameter d_{c}/d of the hexagon air-hole varies from 0.40 to 0.60 at 0.05 interval. We can see that the dispersion depends strongly on wavelength. With the increase of wavelength, the waveguide GVD first increases sharply from a negative value at shorter wavelength, and after a quite gentle variance near the centre of a guiding band, it rises steeply from somewhere within the bandgap as shown in Fig.3(b). These large values of the dispersion (normal at the shorter-wavelength band edge and anomalous at the longer-wavelength band edge) from the Kramers–Kronig relation, is inherent to any optical structure that has relatively sharp transmission features.

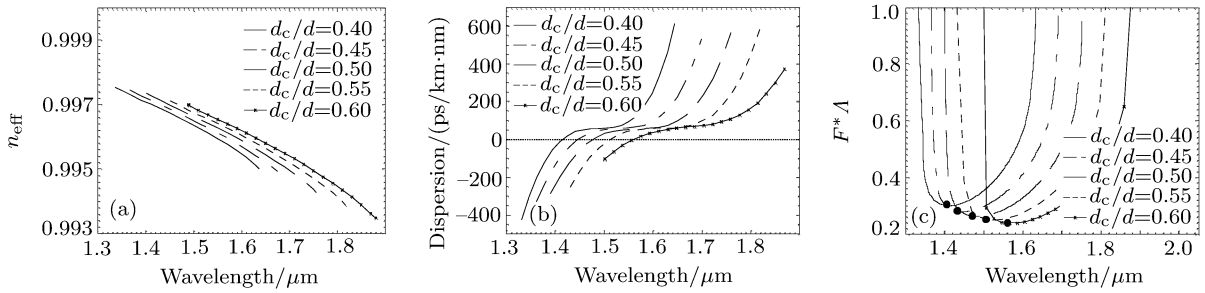


Fig.3. Modal dispersion (a), waveguide GVD (b), and normalized interface field intensity (c) of the fundamental mode of HC-PBGFs with $d_c/d = 0.40, 0.45, 0.50, 0.55, 0.60$. The solid circles in (c) indicate the position of λ_0 for each design.

It is found that with the increase of d_c/d, the dispersion curve shifts towards longer wavelength, as well as the corresponding λ_0, because from the bandgap diagram as shown in Fig.4, with the increase of d_c/d, the bandgap shifts left lower, in other word, it goes toward longer wavelength. At the same time, the bandgap width also witnesses a small increase as shown in Fig.3(a). Particularly interesting is that as d_c/d rises, λ_0 increases by about 150nm, and it takes the following values respectively: $\lambda_0 = 1.406\,\mu$m, $1.433\,\mu$m, $1.471\,\mu$m, $1.506\,\mu$m, and $1.558\,\mu$m. In order to illustrate the rationality of the designs, a relative measure of the scattering loss factor F as a function of wavelength is shown in Fig.3(c), and the positions of λ_0 are especially emphasized by solid circles. It is surprisingly found that the normalized interface field intensity $F\Lambda$ decreases by about 21.5% with d_c/d increasing from 0.4 to 0.6, and that the bandgap width simultaneously increases, which implies the advantages of this method in real applications. However, since the change of geometric structure is so small that it is difficult to obtain the required value of d_c/d during the drawing of fibres.

In addition, Fig.3(b) also indicates that with the increase of d_c/d, the dispersion curve varies more gently, suggesting the possibility of controlling the dispersion slope by varying d_c/d, which is important to practical application.

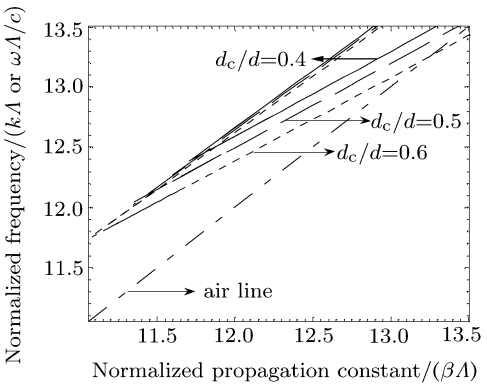


Fig.4. Photonic bandgap diagram for $d_c/d = 0.4$ (solid line), $d_c/d = 0.5$ (dashed line) and $d_c/d = 0.6$ (dotted line).

The dispersion vs. wavelength for different Λ is presented in Figs.5(a) and 5(b), Λ varies from $4.1\,\mu$m to $4.9\,\mu$m, which is the optimized range in fibre fabrication at present.

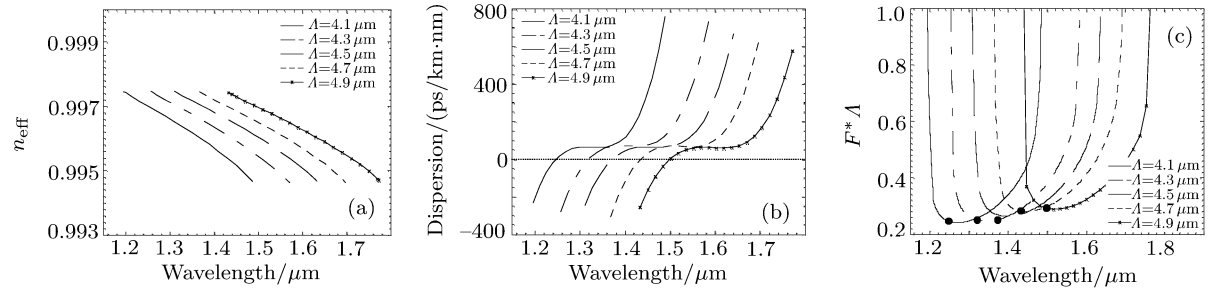


Fig.5. Modal dispersion (a), waveguide GVD (b), and normalized interface field intensity (c) of the fundamental mode of HC-PBGFs with Λ=4.1, 4.3, 4.5, 4.7, 4.9 μm. The solid circles in (c) indicate the position of λ_0 for each design.

It can be seen that as Λ increases, the dispersion curve goes toward longer wavelength, so does λ_0. According to the scaling law, with the increase of $\Lambda/\Lambda_{\rm ref}$, where $\Lambda_{\rm ref}$ is reference hole pitch, the operation wavelength shifts toward longer wavelength and the range of operation wavelength is broaden as shown in Fig.5(a). From Fig.5(b) we can see that the slope at larger Λ is smaller, so the scaling factor $\Lambda/\Lambda_{\rm ref}$ can be used to modify the slopes of the dispersion curves. Figure 6(b) also shows that λ_0 takes respectively 1.248 μm, 1.321 μm, 1.374 μm, 1.433 μm, and 1.499 μm for $\Lambda = 4.1, 4.3, 4.5, 4.7$, and 4.9 μm, increasing by about 250 nm. Similarly $F\Lambda$ vs wavelength for different Λ is given in Fig.5(c), and the solid circles indicate λ_0 for each case. It is found that the normalized interface field intensity at λ_0 for the fibre with $\Lambda = 4.1\,\mu$m is 1.18 times larger than that for the fibre with $\Lambda = 4.9\,\mu$m, which tells us that λ_0 could be controlled by varying Λ at the expense of increasing loss by about 18.29%.

In the process of fibre production, especially for some special fibres, changing the refractive index n of substrate by doping other material is an usual method, since doping often happens in the whole silica, no mechanical and thermal match excite, it could be easily realized in practice, therefore it is necessary to study the effect of n on the dispersion. Figures 6(a) and 6(b) show the variance of dispersion with wavelength for different n, n increases from 1% to 4% at 1% intervals.

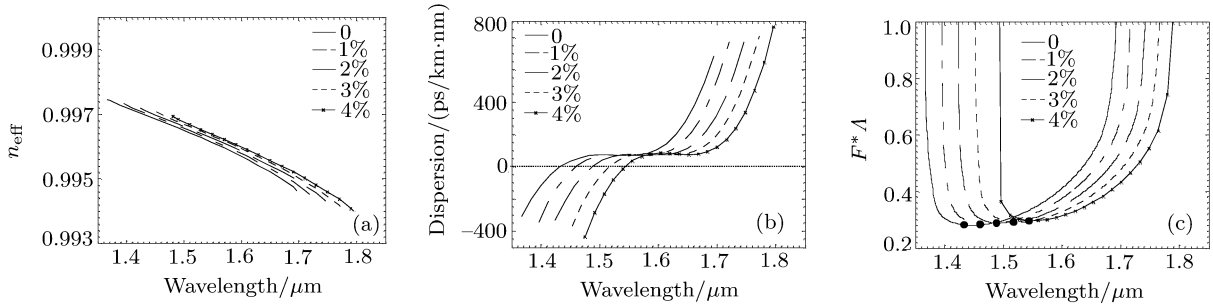


Fig.6. Modal dispersion (a), waveguide GVD (b), and normalized interface field intensity (c) of the fundamental mode of HC-PBGFs with different n. The solid circles in (c) indicate the position of λ_0 for each design.

The dispersion is seen to go toward longer wavelength due to similar variance of bandgap shown in Fig.4, at the same time, λ_0 experiences an increase from 1.433 μm to 1.547 μm for an increase 4% in the refractive index. Figure 6(c) shows that the normalized interface intensity at λ_0 indicated by the solid circles, is only 1.054 times larger when the refractive index increases by 4%, in other words, the loss increases by only about 5.4% during this process, which is no larger than that obtained by the above two other methods, therefore, it is safe to say that in this case varying λ_0 by 114 nm could be achieved with less increase in loss.

Normalized thickness of core rings T plays an important role on the fibre modes, properly selected T can largely reduce loss by suppressing surface modes, thus its influence on dispersion was also considered as shown in Figs.7(a) and 7(b). Figure 7(b) tells us that as T increases, the dispersion also goes toward longer wavelength, during the increase of T from 0.40 to 0.60, λ_0 rises by 45 nm from 1.420 μm to 1.465 μm. But larger T is accompanied by larger loss, which can be revealed by solid circles in Fig.7(c). It is indicated that the normalized interface intensity for T=0.6 is 1.12 times larger than that for T=0.4, implying that moving λ_0 by 45 nm can be realized with 12% increase of the loss. Though λ_0 can be moved toward longer wavelength further by increasing T, this will correspondingly increase the loss and reduce the transmission bandwidth.[16] In addition, Fig.7(b) also indicates that with the increase of T, the dispersion curve varies more gently, suggesting the possibility of controlling the dispersion slope by varying T.

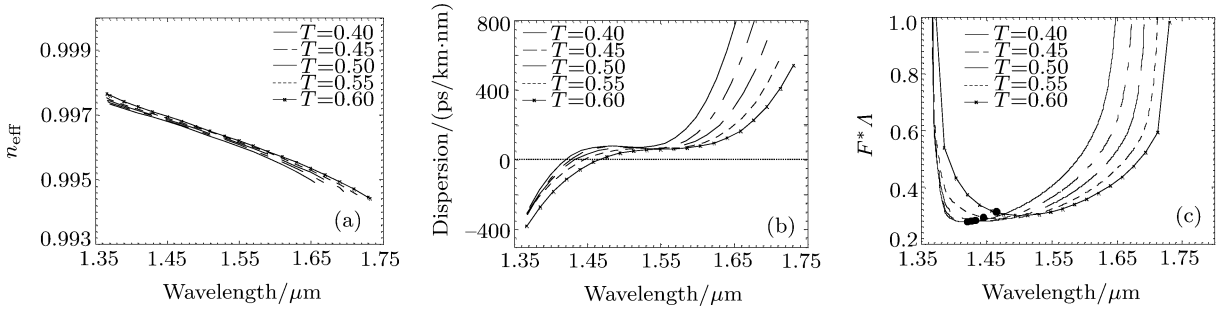


Fig.7. Modal dispersion (a), waveguide GVD (b), and normalized interface field intensity (c) of the fundamental mode of HC-PBGFs with T=0.40, 0.45, 0.50, 0.55, 0.60. The solid circles in (c) indicate the position of λ_0 for each design.

Figures 8(a) and 8(b) show modal dispersion and waveguide GVD for the fundamental mode of the HC-PBGF, where the hole diameter to pitch ratio d/Λ is taken as a parameter. The larger the value of d/Λ is, the smaller the dispersion slope is. And with decrease of d/Λ the bandgap together with λ_0, moves toward longer wavelength, and the width of bandgap becomes more narrower as shown in Fig.8(a). And from Fig.8(b), the dispersion slopes both at the centre and at the bandgap edge of PBG get more steeper. With d/Λ decreasing from 0.98 to 0.95, λ_0 shifts about 623nm, spanning from 1.433 μm to 2.056 μm, the normalized interface field intensity at λ_0 for $d/\Lambda = 0.95$ is 1.685 times larger than that for $d/\Lambda = 0.98$ as shown in Fig.8(c), indicating that a shift of 623 nm in λ_0 will increase the loss by 68.5%. At the same time, bandwidth becomes more and more narrow due to decreasing of air-filling fraction as shown in Fig.8(a). So tuning λ_0 by decreasing the value of d/Λ is unworthy in practice.

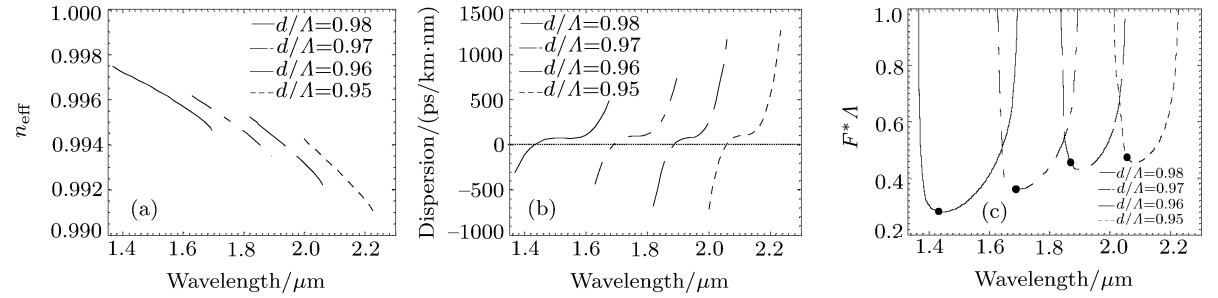


Fig.8. Modal dispersion (a), waveguide GVD (b), and normalized interface field intensity (c) of the fundamental mode of HC-PBGFs with d/Λ=0.98, 0.97, 0.96, 0.95. The solid circles in (c) indicate the position of λ_0 for each design.

4. Conclusion

The dispersion properties of feasible HC-PBGFs with cores formed by omitting 7 central cells were systematically studied by full-vector FEM. Simulations show that with the increase of wavelength, waveguide GVD changes rapidly near the band edge, and has a quite gentle variance near the centre of a guiding band due to PBG effects. Detailed analysis shows that zero dispersion wavelength could be changed by respectively varying rounded diameter of air holes, pitch, refractive index, normalized thickness of core rings, and hole diameter to pitch ratio, while keeping other parameters the same. Comparing the above five strategies, though separately varying the rounded diameter and the thickness of core ring could shift zero wavelength by respectively about 150nm and 45nm at expense of increasing loss by only 21.5% and 12%, we are difficult to get the above parameters within so tiny range in practical drawing of PGBFs, on the other hand, it is possible in practice to respectively alter the pitch and refractive index to shift zero wavelength by about 250nm and 114nm at sacrifice of increasing loss by 18.29% and 5.4%. And despite of 623nm movement of zero wavelength, varying hole diameter to pitch ratio is not worthy because they each induces

large increase of loss and narrowness of transmission bandwidth.

In addition, altering rounded diameter of air holes or pitch or normalized thickness of core rings can control the dispersion slope. In practice, proper method is determined by the producing process of HC-PBGFs.

References

[1] Birks T A, Russell P S J, Atkin D M and Shepherd T J 1995 *Electron. Lett.* **31** 1941

[2] Cregan R F, Mangan B J, Knight J C, Birks T A, Russell P St J, Roberts P J and Allan D C 1999 *Science* **285** 1537

[3] Mi Y, Hou L T, Zhou G Y, Wang K, Chen C, Gao F, Liu B W and Hu M L 2008 *Acta Phys. Sin.* **57** 3583 (in Chinese)

[4] Yuan J H, Hou L T, Zhou G Y, Wei D B, Wang H Y, Dong S R, Wang Q Y, Liu B W and Hu M L 2008 *Acta Phys. Sin.* **57** 4230 (in Chinese)

[5] Benabid F, Knight J C, Antonopoulos G and Russell P St J 2002 *Science* **298** 399

[6] Ouzouno D G, Ahmad F R, Müller D, Venkataraman N, Gallagher M T, Thomas M G, Silcox J, Koch K W and Gaeta1 A L 2003 *Science* **301** 1702

[7] Ouzounov D G, Hensley C J, Gaeta A L, Venkateraman N, Gallagher M T and Koch K W 2005 *Opt. Express* **13** 6153

[8] Benabid F, Knight J C and Russell P St J 2002 *Opt. Express* **10** 1195

[9] Knight J C, Arriaga J, Birks T A, Ortigosa-Blanch A, Wadsworth W J and Russell P St J 2000 *IEEE Photon. Technol. Lett.* **12** 807

[10] Lægsgaard J, Roberts P J and Bache M 2007 *Opt. Quant. Electron.* **39** 995

[11] Lægsgaard J, Mortensen N A, Riishede J and Bjarklev A 2003 *J. Opt. Soc. Am.* B **20** 2046

[12] Obayya S S A, Rahman B M A and El-Mikati H A 2000 *J. Lightwave Technol.* **18** 409

[13] Wang J, Lei N G and Yu C X 2007 *Acta Phys. Sin.* **56** 946 (in Chinese)

[14] Roberts P J, Couny F, Sabert H, Mangan B J, Willliams D P, Farr L, Mason M W, Tomlinson A, Birks T A, Knight J C and Russell P St J 2005 *Opt. Express* **13** 236

[15] Roberts P J, Willliams D P, Mangan B J, Sabert H, Couny F, Wadsworth W J, Birks T A, Knight J C and Russell PSt J 2005 *Opt. Express* **13** 8277

[16] Amezcua-Correa R, Broderick N G R, Petrovich M N, Poletti F and Richardson D J 2006 *Opt. Express* **14** 7974

[17] Roberts P J, Willliams D P, Mangan B J, Sabert H, Couny F, Wadsworth W J, Birks T A, Knight J C and Russell P St J 2005 *Opt. Express* **13** 8277

[18] Amezcua-Correa R, Gérôme F, Leon-Saval S G, Broderick N G R, Birks T A and Knight J C 2008 *Opt. Express* **16** 1142